

D2
N79-27072

A STUDY OF COURSE DEVIATIONS DURING CROSS-COUNTRY SOARING

Steven M. Sliwa
Langley Research Center

David J. Sliwa
University of Illinois at Urbana-Champaign

ABSTRACT

Several models are developed for studying the impact of deviations from course during cross-country soaring flights. Analyses are performed at the micro-strategy and macro-strategy levels. Two types of lift sources are considered: concentrated thermals and thermal streets. The sensitivity of the optimum speed solutions to various model, piloting and performance parameters is evaluated. Guides are presented to provide the pilot with criterions for making in-flight decisions. In general, course deviations are warranted during weak lift conditions, but are less justifiable with moderate to strong lift conditions.

INTRODUCTION

There have been many attempts to develop optimum piloting strategies for the vertical plane of cross-country soaring (for example, references 1 through 5), which basically yield an optimal airspeed given the airmass characteristics, but little has been done with the horizontal plane. References 6 through 8 point out that substantial departures from the optimum speed-to-fly result in small degradations in achieved speed. In fact, the biggest contributing factors influencing average speed are maximizing the achieved rate-of-climb in lift and minimizing the atmospheric sink rate between regions of lift. So it seems that cross-country soaring performance is most influenced by the pilot's decisions made in the horizontal plane.

This paper will address itself to developing some models reflecting typical course deviation decisions a pilot is likely to be confronted with during a cross-country soaring flight. The accompanying analysis should provide guidelines for the pilot to rationally select flight paths which optimize the anticipated lift conditions. Two types of convective lift conditions are considered: soaring conditions where the regions of lift are small relative to the distance flown (circling required) and conditions where the regions of lift are of the order of the distance flown (thermal street flying). In addition, two categories of models are investigated. Micro-strategy models are used to analyze the choice of lift along a desired course line. Macro-strategy models are used for studying the influence of choosing a course line to a goal.

The analysis contained herein assumes parabolic performance polars with numerical examples computed for parameters typical of a modern standard class sailplane. The pilot is assumed to fly at the optimal airspeed for all course choices since perturbations are assumed to have a minor effect. Since final glides are not considered and potential energy is conserved, all models begin and end at the same altitude, cloudbase. Furthermore, all solutions neglect survivability, i.e., they assume the pilot will complete the task no matter which choices are made. Finally, all situations assume that the pilot is far from a ground referenced goal and that the lift is not ground referenced so the influence of wind can be neglected.

LIST OF SYMBOLS

A	Parasitic drag factor, $\frac{1}{2V_o^2(L/D)_{\max}}$
B	Induced drag factor, $\frac{V_o^2}{2(L/D)_{\max}}$
D	Distance on course to lift source goal for thermal street model
d	Distance on course to lift source goal for thermal models
d'	Projected distance of alternate lift source onto course line, Fig. 1
F ₁ , F ₂	Intermediate calculation variables
f	Intermediate calculation variable
h _{CL}	Altitude gained climbing in street lift
h _{CR}	Altitude lost cruising between streets
\dot{h}	Average rate-of-climb while circling in thermals
\dot{h}_s	Rate-of-climb averaged while cruising thermal street lift
K	Intermediate calculation constant, defined in Appendix C, Equation 3
K'	Intermediate calculation constant, defined in Appendix C, Equation 10
(L/D) _{max}	Equivalent to maximum glide ratio in still air
ℓ	Distance flown along street, Fig. 12
ℓ*	Distance to fly along street for optimum time

l'	Distance to fly along street for time equal to not making course deviation
l/D	Non-dimensionalized distance to fly along street, break-away point
m	Slope of tangent line
n	Length of second leg of course deviation, Fig. 12
R	Total distance of a cruise/climb street cycle
R_{CL}	Distance of climb phase of a street cycle
R_{CR}	Distance of cruise phase of a street cycle
Q_i	Value of defining polynomial for i th iteration
s	Total deviation distance of using a street parallel to course line, Fig. 9
s', s_1, s_2	Distance of individual legs of course deviation, Fig. 9
s/D	Deviation distance ratio of parallel street model, Fig. 9
T_D	Time to fly glide/climb thermal cycle on course
T_{ln}	Time to fly course deviation
V	Airspeed while cruising, knots
V^*	Optimum speed-to-fly between lift, knots
V_i^*	Guess of V^* during i^{th} iteration, knots
V_s^*	Sink rate flying at an airspeed of V^* , knots
V_{at}	Average vertical sinking velocity of atmosphere between lift, knots
V_{CL}	Airspeed while climbing in a street, knots
V_{CR}	Required airspeed to cruise in street lift and maintain constant altitude, knots
V_D, V_l, V_n	Airspeed along legs D, l, n respectively

V_G	Average ground speed after a complete glide/climb thermal cycle, knots
V_{GS}	Average ground speed after a complete glide/climb thermal street lift cycle, knots
V_{MIN}	Airspeed for minimum sink rate, knots
V_O	Speed at which $(L/D)_{max}$ occurs, knots
V_S	Sink rate flying at airspeed V , knots
V_{sn}	Sink rate flying at airspeed V_n , knots
W, X, Y, Z	Geometry labels for course deviation models
x	Total deviation distance, Fig. 1
x_1, x_2	Deviation distance legs, Fig. 1
x/d	Deviation distance ratio
y	Distance between parallel street and course line, Fig. 9
y/d	Spacing distance ratio
ζ	Ratio of average rate-of-climb on course to average rate-of-climb along course deviation
η	Ratio of average atmospheric sink rate between lift sources to average rate-of-climb in lift
σ	Ratio of average ground speed on course deviation in augmented lift to ground speed achieved on course with average lift conditions
ϕ	Angle between thermal street and course line
ψ	Angle of thermal model course deviation

PRESENTATION OF RESULTS

Thermal Models

Micro-Strategy

The first case considered is depicted in figure 1. It represents a frequent decision confronting the pilot during cross-country soaring. The pilot,

after departing the thermal at X at cloudbase, must choose between staying on course along path XZ and achieving the average rate-of-climb for that time of day at thermal Z or deviating along XY to the thermal at Y, which looks as if it might yield a higher achieved rate-of-climb. Then the pilot returns to the course after deviating to Y by flying to thermal Z. Given the geometry, the question remains how much greater must be the rate-of-climb at thermal Y than the rate-of-climb at thermal Z to yield the same time for both the direct course and the extended route.

Figure 2 shows the result for a sailplane representative of the standard class. The required rate-of-climb in the thermal at Y is plotted against the non-dimensional deviation distance ratio for a variety of average lift conditions assuming the pilot flies the optimum airspeed, the calculation of which is shown in Appendix A. The curves in figure 2 can be treated as time boundaries. Points to the above and left of a curve indicate that a deviation would be faster than staying on course whereas points to the bottom and right represent conditions for which staying on course would be more profitable.

The importance of deviating for minor gains in lift when the conditions are weak is shown by examining the curve for 1 knot average rate-of-climb on course. A 25% course elongation requires a little over 2 knots rate-of-climb in the thermal at Y. If the expected rate-of-climb in Z were 4 knots (moderate lift conditions), a 25% course deviation ratio would need to have an achieved rate-of-climb better than 15 knots to result in the same time to the top of the thermal at Z. The implication is that when lift conditions are weak (1-2 knots average rate-of-climb), course deviations would be advantageous for modest gains in lift. However, for moderate to strong lift conditions (4 knots and above average rate-of-climb), sizeable gains in lift will permit only minor deviations from the course line.

This result is further emphasized in figure 3 where the deviation distance ratio is plotted against a non-dimensionalized lift ratio for a number of lift conditions. The weak conditions warrant substantial deviation distance ratios even in non-dimensional form while, in contrast, the stronger conditions begin to coincide upon a boundary requiring large lift ratios for any appreciable distance ratio.

The influence of sailplane performance upon the pilot's decisions is shown in figure 4. Rate-of-climb required at thermal Y is plotted as a function of deviation distance ratio for three classes of sailplanes. Sailplane A is the standard class aircraft considered previously; sailplane B represents a one-design sport class; and aircraft C represents a sailplane in the open class. It is readily apparent that sailplane performance has a minor effect on the pilot's willingness to deviate from course. However, there is a trend for sailplanes of lesser performance to be willing to make slightly greater course deviations.

The previous curves were developed with an assumed average atmospheric subsidence equal to 20 percent of the rate-of-climb (reference 9). As expected, slight course extensions with this model can be justified with reduced sink rate

(figure 5). However, the influence of sink rate on the pilot's decision to deviate from course, assuming that both flight paths undergo the same average sink rate, is negligible.

An important variable in the geometry shown in figure 1 is d'/d . It impacts the performance of the extended course by determining how much of the altitude to be regained will be done in the stronger thermal at Y. The generalized results for d'/d of .25, .5, and .75 are shown in figure 6 for average lift conditions of 2 knots and 6 knots. It is readily apparent from figure 6 that substantially larger course deviations can be justified with larger values of d'/d . The greater the distance between X and Y for a given deviation distance ratio, the greater the altitude which is gained in the stronger lift at Y, thereby increasing the achieved speed.

The net result of the foregoing analysis is that the deviation angle, Ψ , should be kept as small as possible. This is especially true for moderate to strong lift conditions. This result is in basic agreement with the macro-strategy model presented in reference 10 which is of similar format to the micro-strategy model considered here.

It should be noted that the preceding results can be directly applied to a more generalized model including multiple glide/circle cycles along the course line segments XZ and XY. This is true as long as the deviation flight path includes only one glide/circle cycle along YZ. The reason multiple thermals do not affect the analysis is due to the simplification that net ground speed is a function of achieved rate-of-climb, so the time to reach cloudbase at the end of a segment will be the same no matter how many thermals are used.

The results of another micro-strategy analysis are shown in figure 7. Speed ratio, achieved ground speed with vertical air motion between thermals normalized by achieved ground speed with no vertical air motion between thermals, is plotted against sink ratio, which is the ratio of average vertical air motion between lift sources to achieved rate-of-climb in lift for a variety of lift conditions. Negative sink ratios are indicative of what pilots call "reduced sink," i.e., positive vertical air motion too weak to yield a positive rate-of-climb, but still result in a reduction of the rate at which altitude is lost. The curves in figure 7 are continued in the negative sink ratio direction until "zero sink" (the point at which the net altitude loss during cruising is zero) is achieved.

Speed ratios greater than 1 can be interpreted as deviation distance ratios. For example, a speed ratio of 1.1 implies that a pilot could deviate from his straight line course by 10% and still have the same achieved ground speed for a complete glide/circle cycle. If the pilot deviates from course any less, for the indicated lift and sink conditions, a net gain in cross-country speed will result. These results reiterate the necessity for minimizing sink rate by making minor deviations during inter-thermal cruise to optimize the achieved cross-country performance.

Macro-Strategy

Macro-strategies involve the choice of courses to a desired goal rather than the flight path selection to individual sources of lift. Macro-strategies are used to fly through regions of improved lift conditions. So once a macro-strategy is developed, an undetermined number of micro-strategies are used to fly the prescribed course.

The results of the thermal macro-strategy model are shown in non-dimensional form in figure 8. Speed ratio is plotted as a function of lift ratio for a variety of average lift conditions. As before, the non-dimensionalized speed ratio can be interpreted as the deviation distance ratio boundary required for equal time to reach the goal. It is immediately obvious, by comparing figures 3 and 8, that decisions on the macro-strategy level have a much greater impact upon the achieved cross-country soaring performance than decisions at the micro-strategy level. A lift ratio of 2.0 yields more than twice the speed ratio for all lift conditions for the macro-strategy case in comparison with the micro-strategy case. The importance of choosing courses that will pass through more favorable sectors is of greater importance for weak conditions as opposed to moderate or strong thermal conditions.

As before, although sailplane performance and sink between thermals will affect achieved groundspeed, they have little influence upon the pilot's decision of when to make course deviations.

Street Models

Many times the pilot will have occasion to utilize convective lift while cruising along course line. This condition where the regions of lift make up a substantial portion of the flight path is usually referred to as streeting. Making effective use of these large regions of lift usually involves speeding up in sink and slowing down in lift. There have been several analyses of this mode of flying, for example, references 2 through 5 and 11 through 14. In this paper, however, simplified and conservative control laws have been implemented for studying thermal street flying. For the most part, the pilot flies at the speed for minimum sink rate while in lift until cloud base is reached, at which time the pilot speeds up and flies so as to maintain altitude. The pilot cruises between lift as dictated by the equations of Appendix B. As it turns out, this procedure is not far from the optimum as demonstrated in reference 5.

Micro-Strategy

The first model to be considered is shown in figure 9. The pilot has reached cloud base at Point W and is trying to get to Point Z. He must decide if flying straight to Z or deviating to use the thermal street along XY will yield the fastest time to cloud base at Point Z. It is assumed that

the pilot is capable of achieving an average rate-of-climb along \overline{XY} equal to half the rate-of-climb obtainable from circling in thermals on course $\frac{h_s}{h} = 0.5$.

Optimal inter-lift cruising speeds are obtained from Appendices A and B. The pilot uses the control law previously mentioned for cruising in the lift along \overline{XY} .

The results are shown in figures 10 and 11 for this model. Boundaries of deviation distance ratio, s/D , yielding the same time to cloudbase at Z are plotted against average lift conditions for a variety of street length ratios, s'/D , in figure 10. As anticipated, the geometry of the situation confronting the pilot has a much greater influence on his decision than rate-of-climb, sail-plane performance or inter-lift sink. Obviously, the greater the length of \overline{XY} (s'), the greater the distance the pilot should be willing to transverse to improve his cross-country soaring performance. Course deviations for weak conditions can be about 10% longer than for moderate to strong conditions.

A more convenient way for the pilot to picture how far of a course deviation is warranted is shown in figure 11. It is a plot of curves showing allowable spacing-distance ratio, y/D , against achieved rate-of-climb for street length ratios of 0.2 and 0.8. Spacing distance ratios of about 35% and 45% respectively are justified for weak conditions while spacing distance ratios of about 25% and 35% are allowed for moderate to strong thermal conditions.

The second micro-strategy thermal street model is shown in figure 12. The pilot has just reached cloudbase in a thermal at X and desires to reach cloudbase at the thermal at point Z . He must decide between flying directly on course or deviating to use the street along \overline{XY} and then flying to Z . It is assumed that the average vertical atmospheric velocity along \overline{XY} is equivalent to that which would yield half the rate-of-climb from thermalling at points X or Z . The pilot flies along \overline{XY} at the speed which yields no net altitude change and then flies along \overline{YZ} at the speed-to-fly indicated by the methods of Appendix A.

Prior to analyzing the model, it is necessary to determine the optimum method of flying the street and the sensitivity to variations from the optimal procedures. Figure 13 is a series of plots showing speed ratio, i.e., the speed obtained by deviating to fly the street at angle ϕ normalized by the speed obtained flying straight ahead in the classical circle/glide manner, as a function of breakaway distance ratio, l/D , for a variety of street angles. Speed ratios greater than one correspond to flight path extensions which would yield a faster time to cloudbase at Z than the straight-ahead choice. Figure 13 shows the following: 1) there are many ways to fly the thermal street so as to obtain a speed ratio greater than 1; 2) there exists, for thermal street angles less than about 60° , an optimal distance along the street to break away and begin flying toward Z to optimize speed ratio; 3) this optimum breakaway distance is highly sensitive to street angle and not very sensitive to rate-of-

climb; 4) the greatest speed ratios are obtained with small angles and weak lift conditions; and, 5) optimum speed ratio is highly sensitive to breakaway point for weak lift and small street angles.

The breakaway point which yields equal time to fly the street and the straight ahead glide/circle cycle and the breakaway point for the optimum time by flying the street is analytically derived in Appendix C. The locus of breakaway points for equal time (straight ahead versus deviating along the street), l'/D , and optimum time, l^*/D , is shown as a function of obtainable average rate-of-climb thermalling for a variety of street angles in figure 14. The optimum breakaway point from the street is not greatly affected by average rate-of-climb whereas the breakaway point for equal time can be extended along the street substantially during weaker conditions as compared with moderate to strong lift conditions. As expected, figure 15, which shows obtainable speed ratio for a variety of thermal street angles, indicates that the largest gains in speed ratio from flying the thermal street are possible with weak conditions and/or small thermal street angles.

The influence of street angle on breakaway points for optimum time and equal time is shown in figure 16. It is clear that deviating along a street is not beneficial for street angles of 60° or more. In addition, it can be observed that there is a very large margin between the locus of points equal time and optimum time, indicating that the pilot can choose a large number of breakaway points and still improve his performance. Even so, it would probably be beneficial for the pilot to study this plot and develop rules of thumb for deciding upon the optimum breakaway point given a geometry and lift condition. For example, neglect obtainable average rate-of-climb thermalling and just decide by reference to street angle-- 15° fly an l/D of 90%; 30° fly an l/D of 70%; 45° fly an l/D of 50%; and 60° and greater fly straight ahead ignoring the street. The magnitude of the benefits to be obtained from deviating along streets as a function of street angle is demonstrated in figure 17.

Macro-Strategy

The equations for studying the effect of streeting are developed in Appendix B. The macro-strategy model to be considered is basically the same as considered previously except that some portion of the course deviation is under the influence of convective lift. As before, it is assumed that the average vertical air velocity encountered while cruising is equivalent to half the achieved rate-of-climb in thermals.

It is assumed that after a long enough stretch of cloud street flying that the net change in altitude is constrained to be zero. This is valid only at the macro-strategy level because the pilot might be willing, in the short term, to tolerate slow losses of altitude in order to make progress along the desired course. The required ratio of distance flown while climbing to total distance covered is plotted in figure 18 against achieved rate-of-climb in thermals for 3 sailplanes. The sport class sailplane requires considerably more of the flight path in lift than the other two classes studied. It should also be remembered that

this assumes static equilibrium flight and neglects the performance differences due to the dynamics of pulling up and pushing over, which should increase the differences between classes. Some of these dynamic effects have been studied previously, for example, reference 14.

The importance of deviating from course to be able to cruise while climbing is shown in figure 19. Speed ratio is shown as a function of rate-of-climb achievable by thermalling for three ratios of distance covered while climbing in thermal streets to total distance covered. Here it is assumed, that in order to have no net change in altitude after a long period of time, one of two approaches must be taken: 1) if there is more lift available than necessary to maintain altitude, the excess will be used to increase speed at cloudbase until no net change in altitude will occur; or, 2) if there is not enough lift available to maintain altitude, the pilot will circle to cloudbase at the end of the cruise at the average rate-of-climb expected in thermals at that time. The fourth curve is a locus of points obtained from figure 18 showing the achieved performance if the ratio of distance covered climbing to total distance covered were at the correct value to yield no net altitude change from climbing by cruising at the speed for minimum sink and cruising between lift at the appropriate speed-to-fly (Appendix B).

Several assumptions have been made during the development of the street flying analyses which need to be considered. The authors have studied the influence of sailplane performance and inter-thermal sink and found that, although the cross-country performance may be significantly affected, the pilot's decision in regards to non-dimensionalized course deviations is not altered. The assumption that the average vertical atmospheric velocity encountered while climbing is 50% that of the vertical air velocity obtainable in thermals at the time does influence various parts of the analysis. It is felt, however, that this does not have a major impact upon the trends demonstrated in this paper. Furthermore, neglecting winds in these analyses probably would affect the decisions a pilot would make during cross-country street flying. Thermal streets are usually fostered by gentle winds and the inclusion of this factor warrants further research. As exemplified in reference 15, the pilot would probably be willing to make further progress against the wind in streets than the optimum solutions for still air reported herein.

SUMMARY OF RESULTS

Several trends came out of the analysis of the thermal models in this paper. It is apparent that decisions to deviate from course are of much greater significance at the macro-strategy level than the micro-strategy level. A pilot can enhance his performance by choosing sectors of the sky to improve his achieved rate-of-climb. At both the micro- and macro-strategy levels it is clear that substantial deviations from course may be warranted for weak lift whereas when the thermal conditions are moderate or strong, only very minor course deviations can be justified. In all cases, cross-country soaring performance can be augmented by making course deviations with the

smallest possible deviation angles. This indicates that pilots should make course change decisions as soon as possible and be willing to ignore lift not near the course, which is especially true for moderate or strong lift.

A large improvement in average cross-country speed is attainable by cruising while climbing, such as in streeting conditions. In the street models considered, the percentage of the flight path in lift had a big influence upon the achieved performance and pilot's decision criteria. In the case of the parallel street micro-strategy model, streets with spacing distance ratios of 30% or less could be justified to increase the attained cross-country speed. Deviation distance ratios can be extended by about 10% for weak conditions as compared to moderate or strong lift conditions.

The study of streets at an angle to the course line results in some interesting observations. There exists an optimum point of breakaway from the street to minimize the time required to reach the top of the next thermal. This breakaway point is primarily a function of street angle. Although the optimum augmentation of speed is highly sensitive to breakaway point for weak conditions at small street angles, for most combinations of street geometry and lift conditions there exists a range of possible solutions which yields a faster time than the straight ahead glide/circle cycle. It can be shown that cloud streets at an angle greater than 60 degrees are not beneficial and should not be used to improve average ground speed.

CONCLUDING REMARKS

Several assumptions have been made which may affect the applicability of the results reported upon herein. A premise for all the cases studied was that survivability is ignored. Speed was considered as the performance function to be optimized whereas if the pilot was concerned about not being able to complete the flight, altitude conservation would be of prime importance.

A constraint for each exercise was that net altitude loss would be zero; hence, the results are not applicable to final glides. A possible focus of future research may be to study the impact of course deviations upon final glides. Also, it was arbitrarily assumed for the street models that average lift in a street was approximately 50% of the lift found in thermals at that time. This has an obvious impact upon the performance gains of deviating to use streets, but general trends of the analyses are still valid.

A significant limitation of the approach presented in this paper is the assumption implied by considering lift as solely air referenced. This negates the influence of winds for reaching ground referenced goals or lift sources. It is expected that decisions reached during the street analysis will be shifted into the wind. For example, the pilot will probably want to make more progress into the wind while in lift than otherwise indicated by the breakaway point solutions. Since thermal streets are usually formed in light to medium winds, the inclusion of winds in the foregoing analyses is currently being undertaken by the authors.

The models developed in this paper are simplified and general in nature. It is hoped that they or a linear superposition of more than one of them are representative of typical lift geometries a pilot may encounter during a cross-country soaring flight. The results presented in this paper are not meant to be cockpit aids for interpreting the most promising flight paths. Instead, they illustrate the desirability and indicate an approach, for analytically studying typical course selection decisions beforehand, enabling the pilot to more effectively evaluate the potential tradeoffs for arriving upon a more optimal solution while in flight.

APPENDIX A

OPTIMUM SPEED-TO-FLY CALCULATIONS FOR THERMAL MODELS

To facilitate the calculations required in this paper and in other investigations (reference 16), analytical expressions needed to be derived for the familiar inter-thermal speed-to-fly solution (reference 1). Although the defining equations are easily derived and have been presented in numerous publications (for example, references 3 and 5), a closed form analytical solution for calculating numerical results is not generally available in the literature and is given below. The graphical interpretation of the results which is widely used by pilots is shown in figure 20. The first case considered is where the sailplane performance is known and is assumed to be parabolic; the average rate-of-climb in the next thermal is known; the ratio of sink rate between thermals to rate-of-climb in them is known; and the optimum speed-to-fly between the thermals and the corresponding average ground speed is desired. The sailplane performance relation is:

$$V_s = AV^3 + \frac{B}{V} \quad (A1)$$

where

$$A = \frac{1}{2V_o^2(L/D)_{\max}} \quad (A2)$$

$$B = \frac{v_o^2}{2(L/D)_{\max}} \quad (A3)$$

The defining equation can be found from figure 20 or by derivation to be

$$\frac{V_s + \dot{h} + V_{at}}{V} = \frac{d}{dV} V_s \quad (A4)$$

By applying the definition of sink ratio, η , and utilizing equations (A1), (A2), and (A3), equation (A4) becomes the following fourth degree polynomial:

$$V^4 - \frac{\dot{h}(1 + \eta)}{2A} V - \frac{B}{A} = 0 \quad (A5)$$

The root of interest was found to be calculated by the following relations:

$$v^* = \frac{\sqrt{f}}{2} + \sqrt{\frac{-f + \frac{(1+\eta)\dot{h}}{A\sqrt{v}}}{2}} \quad (A6)$$

$$f = \sqrt[3]{F_1 + F_2} + \sqrt[3]{F_1 - F_2} \quad (A7)$$

$$F_1 = \frac{(1+\eta)^2 \dot{h}^2}{8A^2} \quad (A8)$$

$$F_2 = \sqrt{\frac{[(1+\eta)\dot{h}]^4}{64A^4} + \frac{64B^3}{27A^3}} \quad (A9)$$

The average ground speed for a complete glide/circle cycle is given by

$$V_G = \frac{v^* \dot{h}}{AV^{*3} + B/V^* + (1+\eta)\dot{h}} \quad (A10)$$

The second case considered is where the sailplane performance is known in the form as before, the sink ratio can be assumed, the desired average ground speed is known, and the optimum speed-to-fly and the required rate-of-climb given the preceding are to be found. The defining equation can be easily attained from figure 20 by equating the slope of the tangent line,

$$m = \frac{v_s^*}{v^* - (1+\eta)V_G} \quad (A11)$$

to the slope of the sailplane polar found by differentiating equation (A1)

$$\frac{d}{dv} v_s = 3AV^2 - \frac{B}{V^2} \quad (A12)$$

The defining equation for the optimum solution becomes

$$v^{*5} - \frac{3}{2}(1+\eta)V_G v^{*4} - \frac{B}{A}v^* + \frac{B}{2A}(1+\eta)V_G = 0 \quad (A13)$$

Use Newton's method for estimating roots. Let

$$Q_1 = v_1^{*5} - \frac{3}{2}(1+\eta)V_G v_1^{*4} - \frac{B}{A}v_1^* + \frac{B}{2A}(1+\eta)V_G \quad (A14)$$

$$\frac{d}{dV^*} Q_i = 5V_i^{*4} - 6(1 + \eta)V_G V_i^{*3} - \frac{B}{A} \quad (A15)$$

then,

$$V_{i+1}^* = V_i^* - \frac{Q_i}{\frac{d}{dV^*} Q_i} \quad (A16)$$

A good initial guess for V_i^* could arbitrarily be $V_0 + 5(1 + \eta)h$. A fair amount of accuracy can be obtained with just five iterations in this manner. The required rate-of-climb for an average ground speed of V_G is given by the following relation:

$$h = \frac{AV_G V^{*3} + BV_G/V^*}{V^* - (1 + \eta)V_G} \quad (A17)$$

APPENDIX B

OPTIMUM SPEED-TO-FLY CALCULATIONS FOR THERMAL STREETS

The defining relations and a geometric interpretation (figure 21) of the optimum speed-to-fly between lift, given the sailplane performance, the inter-lift sink ratio, the rate-of-climb and the speed at which the lift is transversed (V_{CL}), were presented in reference 5. The defining equation is

$$\frac{d}{dV} V_s = \frac{V_s + h_s + V_{at}}{V^* - V_{CL}} \quad (B1)$$

Assuming a parabolic polar, equations (A1), (A2), and (A3), the following fifth degree polynomial can be derived

$$V^{*5} - \frac{3}{2} V_{CL} V^{*4} - \frac{(1 + \eta)}{2A} h_s V^{*2} - \frac{B}{A} V^* + \frac{B V_{CL}}{2A} = 0 \quad (B2)$$

Newton's iterative method of estimating real roots was used to solve the fifth degree equation for the desired root.

Let

$$Q_i = V_i^5 - \frac{3}{2} V_{CL} V_i^4 - \frac{(1 + \eta)}{2A} h_s V_i^2 - \frac{B}{A} V_i + \frac{B}{2A} V_{CL} \quad (B3)$$

$$\frac{d}{dV^*} Q_i = 5V_i^4 - 6V_{CL} V_i^3 - \frac{(1 + \eta)}{A} h_s V_i - \frac{B}{A} \quad (B4)$$

then

$$V_{i+1}^* = V_i^* - \frac{Q_i}{\frac{d}{dV^*} Q_i} \quad (B5)$$

A good value for the initial guess of V_i^* might arbitrarily be the solution to the thermal model problem developed in Appendix A. A near optimum value for the climbing velocity, V_{CL} , would be the speed for minimum sink rate, V_{MIN} .

$$\frac{d}{dV} V_s = 0 = 3AV^2 - \frac{B}{V^2} \quad (B6)$$

$$V_{\text{MIN}} = \sqrt[4]{\frac{B}{3A}} = v_o \sqrt[4]{1/3} \quad (\text{B7})$$

$$V_{\text{MIN}} = .7598 v_o \quad (\text{B8})$$

The average ground speed for a complete cycle, as pictured in figure 22, is calculated as follows:

$$V_{\text{GS}} = \frac{\dot{h}_s}{3AV^*2 - \frac{B}{v^*2}} + V_{\text{MIN}} \quad (\text{B9})$$

These equations were derived assuming that the net altitude change after each cruise/climb cycle was zero. Referring to figure 22, a relation can be derived to yield the proportion of the flight path which must be under the influence of lift to result in no net altitude change after each cycle ($h_{\text{CR}}/h_{\text{CL}} = 1$).

Starting with

$$h_{\text{CR}} = \frac{R_{\text{CR}}}{V_{\text{CR}}} (v_s^* + \eta \dot{h}_s) \quad (\text{B10})$$

$$h_{\text{CL}} = \frac{R_{\text{CL}}}{V_{\text{CL}}} \dot{h}_s \quad (\text{B11})$$

and

$$\frac{R_{\text{CL}}}{R} = \frac{\left(\frac{R_{\text{CL}}}{R_{\text{CR}}}\right)}{1 + \frac{R_{\text{CL}}}{R_{\text{CR}}}} \quad (\text{B12})$$

The following equation is derived

$$\frac{R_{\text{CL}}}{R_{\text{CR}}} = \frac{\left(\frac{h_{\text{CL}}}{h_{\text{CR}}}\right) \left(\frac{V_{\text{CL}}}{V^*}\right) \left(\frac{v_s^*}{h_s} + \eta\right)}{1 + \left(\frac{h_{\text{CL}}}{h_{\text{CR}}}\right) \left(\frac{V_{\text{CL}}}{V^*}\right) \left(\frac{v_s^*}{h_s} + \eta\right)} \quad (\text{B13})$$

A plot of R_{CL}/R as a function of \dot{h}_s for three sailplanes is shown in figure 18.

In the event that there is a larger proportion of the flight path under the influence of lift than required for no net altitude change, then the pilot needs to cruise at a velocity which gives a sink rate equal to the vertical air velocity to keep from climbing into the cloud. This airspeed can be calculated as follows:

$$V_{at} \equiv V_s = AV^3 + B/V \quad (B14)$$

$$V_{CR} = \frac{\sqrt{f}}{2} + \frac{\sqrt{-f + 2V_s \frac{s}{AVf}}}{2} \quad (B15)$$

$$f = \sqrt[3]{F_1 + F_2} + \sqrt[3]{F_1 - F_2} \quad (B16)$$

$$F_1 = \frac{V_s^2}{2A^2} \quad (B17)$$

$$F_2 = \sqrt{\frac{V_s^4}{4A^4} - \frac{64B^3}{27A^3}} \quad (B18)$$

APPENDIX C

CALCULATION OF BREAK-AWAY POINTS FROM A CLOUD STREET AT AN ANGLE TO THE DESIRED COURSE

Using the geometry defined in figure 12, a relation can be defined to determine the appropriate breakaway points in terms of sailplane performance parameters and atmospheric lift conditions. The first case considered is finding the breakaway point, the distance to be flown along the street, ℓ , to yield the same time to the top of the thermal as Z as by flying directly from X to Z . The time to fly along the street, fly to Z and then climb to cloud-base at Z is given by:

$$T_{\ell n} = \frac{\ell}{V_{\ell}} + \frac{n}{V_n} + \frac{n}{V_n} \left(\frac{V_{sn}}{h} + \frac{h\eta}{h} \right) \quad (C1)$$

$$T_{\ell n} = \frac{\ell}{V_{\ell}} + \frac{n}{V_n} \left(1 + \frac{V_{sn}}{h} + \eta \right) \quad (C2)$$

if

$$K = 1 + \frac{V_{sn}}{h} + \eta \quad (C3)$$

then

$$T_{\ell n} = \frac{\ell}{V_{\ell}} + \frac{n}{V_n} K \quad (C4)$$

Using the Law of Cosines

$$n^2 = D^2 + \ell^2 - 2D\ell \cos \phi \quad (C5)$$

Squaring equation (C4) yields

$$T_{\ell n}^2 - 2\frac{\ell}{V_{\ell}} T_{\ell n} + \frac{\ell^2}{V_{\ell}^2} = \frac{n^2}{V_n^2} K^2 \quad (C6)$$

Substituting equation (C5) into (C6) gives

$$T_{\ell n}^2 - 2\frac{\ell}{V_{\ell}} T_{\ell n} + \frac{\ell^2}{V_{\ell}^2} = \frac{K^2}{V_n^2} \left[D^2 + \ell^2 - 2D\ell \cos \phi \right] \quad (C7)$$

From the definition of completing either route in equal time and from the assumptions of Appendix A, V_n and V_D are equal since they are both calculated based on the thermal at Z, the following can be written:

$$T_{ln} \equiv T_D = \frac{D}{V_n} \left(1 + \frac{V_{sn}}{h} + \eta \right) = \frac{D}{V_n} K \quad (C8)$$

Substituting (C8) into (C7) results in

$$\ell^2 \left(\frac{V_n^2}{V_\ell^2} - K^2 \right) + \ell \left(2DK \right) \left(K \cos \phi - \frac{V_n}{V_\ell} \right) = 0 \quad (C9)$$

If we define the following constant,

$$K' = \frac{V_n}{V_\ell} \frac{1}{K} \quad (C10)$$

then equation (C9) can be solved for the roots as follows

$$\frac{\ell'_1}{D} = 0 \quad (C11)$$

$$\frac{\ell'_2}{D} = \frac{2 (\cos \phi - K')}{1 - K'^2} \quad (C12)$$

The second case considered is the solution for the non-dimensionalized breakaway point, $\frac{\ell^*}{D}$, for minimum time to reach the top of the thermal at Z. Starting with equation (C4) and substituting the square root of equation (C5) into it, the following function is obtained:

$$T_{ln} = \frac{\ell}{V_\ell} + \frac{K}{V_n} \left(D^2 + \ell^2 - 2D\ell \cos \phi \right)^{1/2} \quad (C13)$$

The minimum time solution for T_{ln} is found by differentiating with respect to ℓ and setting it to zero.

$$\frac{d}{d\ell} T_{\ell n} \equiv 0 = \frac{1}{V_{\ell}} + \frac{K}{V_n} \frac{\ell - D \cos \phi}{(D^2 + \ell^2 - 2D\ell \cos \phi)^{\frac{1}{2}}} \quad (C14)$$

Rearranging (C14) and substituting in equation (C10) gives the following quadratic equation:

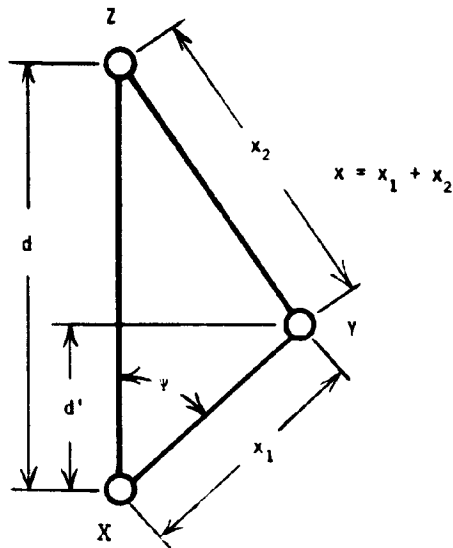
$$\ell^2 (1 - K'^2) + \ell (2D \cos \phi) (K'^2 - 1) + D^2 (\cos^2 \phi - K'^2) = 0 \quad (C15)$$

The root of interest from equation (C15) is

$$\frac{\ell^*}{D} = \cos \phi - \sqrt{\frac{K'^2 (1 - \cos^2 \phi)}{(1 - K'^2)}} \quad (C16)$$

REFERENCES

1. McCready, Paul B.: "An Optimal Airspeed Selector," Soaring, May 1954.
2. Mozdiniewicz, W.: "Cloud Street Flying," Soaring, Vol. 35, No. 11, 1971 pp. 26-27.
3. Irving, F. G.: "Cloud Street Flying," NASA CR-2315, 1972, pp. 274-286.
4. Gedeon, Jozsef: "Dynamic Analysis of Dolphin-Style Thermal Cross-Country Flying," Technical Soaring, Vol. 3, No. 1, 1973.
5. Abzug, Malcolm J.: "A Speed Ring for Cloud Street Flying," Technical Soaring, Vol. 14, No. 1, 1976.
6. Irving, F. G.: "The Effect of Errors in Inter-Thermal Speed on the Average Cross-Country Speed," Technical Soaring, Vol. 3, No. 2, 1973.
7. Schuemann, Wil: "The Price You Pay for MacCready Speeds," Presented at the 1972 Symposium on Competitive Soaring, Soaring Symposia, Cumberland, Maryland, 1973.
8. Teter, Michael P.: "Competition Strategy and Tactics for Beginners," Soaring, August, 1975, pp. 26-28.
9. Johnson, Richard H.: "Cross-Country Soaring," American Soaring Handbook, Soaring Society of America, 1962, Chapter 6, pg. 8.
10. Alleman, Rudolf T.: "Notes on the Dilemma of Deviation from Course Line," Soaring, March, 1962, pp. 12-14.
11. Arho, Risto: "Optimal Dolphin Soaring as a Variation Problem," Technical Soaring, Vol. 3, No. 1, 1973.
12. Arho, Risto: "Some Notes on Soaring Flight Optimization Theory," Technical Soaring, Vol. 14, No. 2, 1974.
13. Metzger, Darryl E. and Hedrick, J. Karl: "Optimal Flight Paths for Soaring Flight," Proceedings of Second International Symposium on the Technology and Science of Low-Speed and Motorless Flight, Cambridge, Mass., 1974.
14. Gedeon, Jozsef: "The Influence of Sailplane Performance and Thermal Strength on Optimal Dolphin-Flight Transition Piloting Techniques," Presented at the XV OSTIV Congress, Rayskala, Finland, 1976.
15. Reichman, Helmut: Cross-Country Soaring: A Handbook for Performance and Competitive Soaring, Thompson Publications, Santa Monica, California, 1978.
16. Sliwa, Steven M.: "A Computer Simulation of Cross-Country Soaring," Soaring, January 1976.



REPRODUCIBILITY OF THE ORIGINAL PAGE IS POOR

Figure 1. - Micro-strategy thermal model.

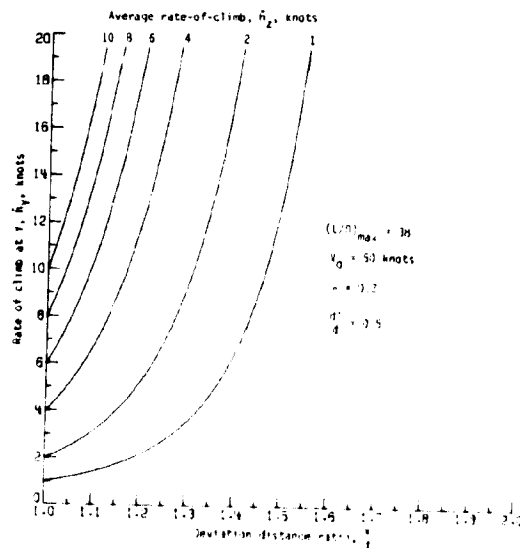


Figure 2. - Required rate-of-climb at Y as a function of deviation distance ratio for micro-strategy thermal model.

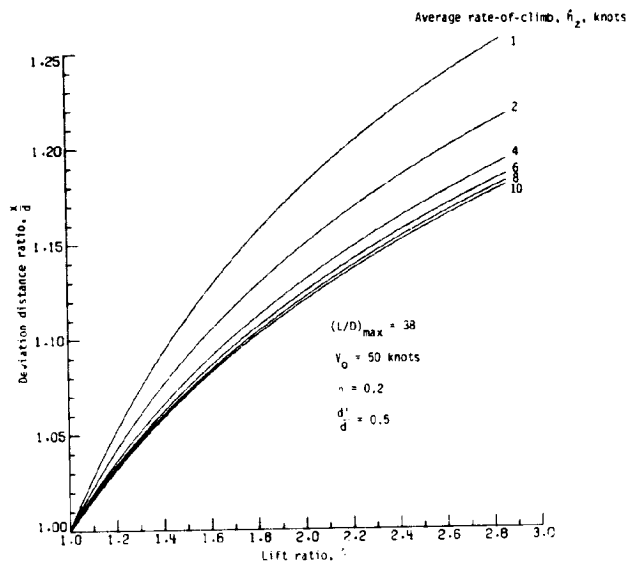


Figure 3. - Deviation distance ratio as a function of lift ratio for micro-strategy thermal model.

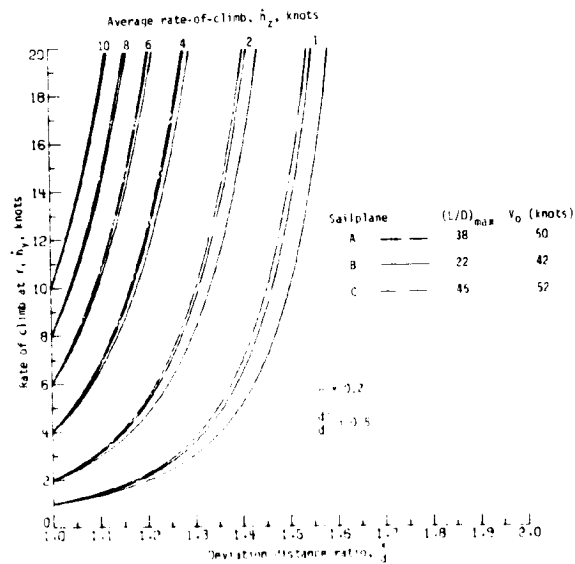


Figure 4. - Required rate-of-climb at Y versus deviation distance ratio illustrating impact of sailplane performance for micro-strategy thermal model.

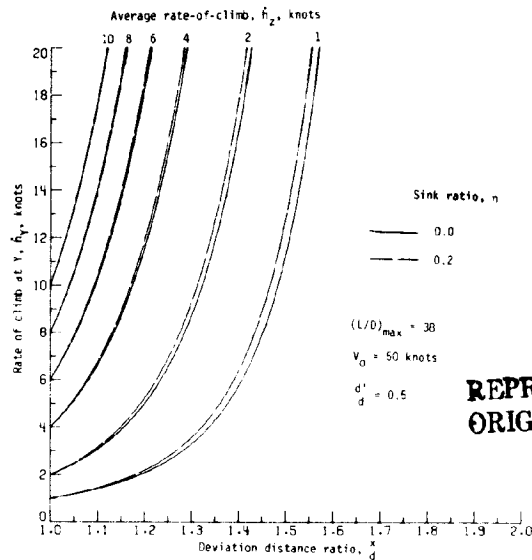


Figure 5. - Required rate-of-climb at Y versus deviation distance ratio illustrating impact of sink ratio for micro-strategy thermal model.

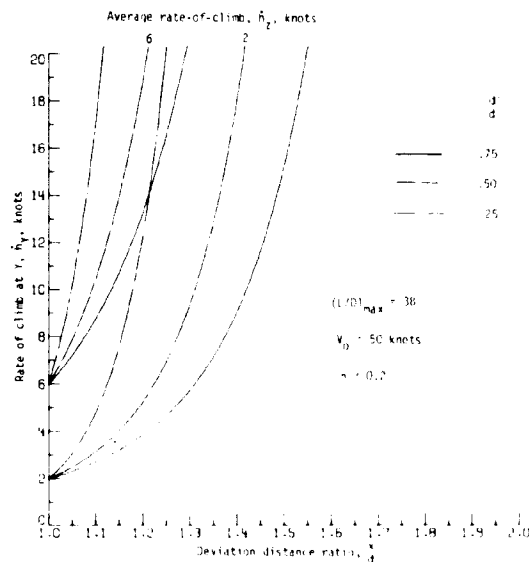


Figure 6. - Required rate-of-climb at Y versus deviation distance ratio illustrating impact of d'/d for micro-strategy thermal model.

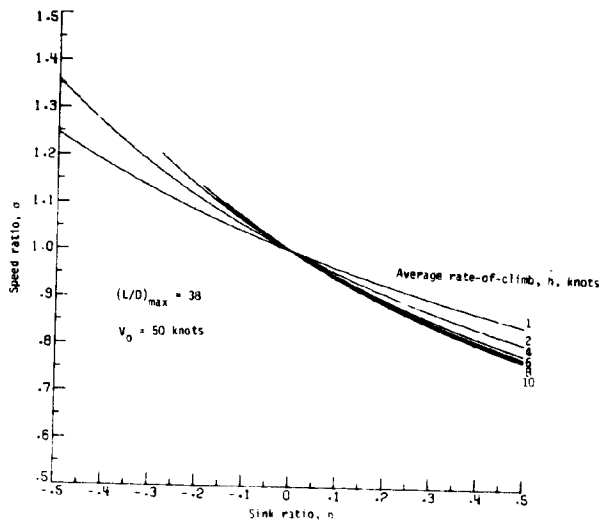


Figure 7. - Speed ratio versus sink ratio for micro-strategy thermal analysis.

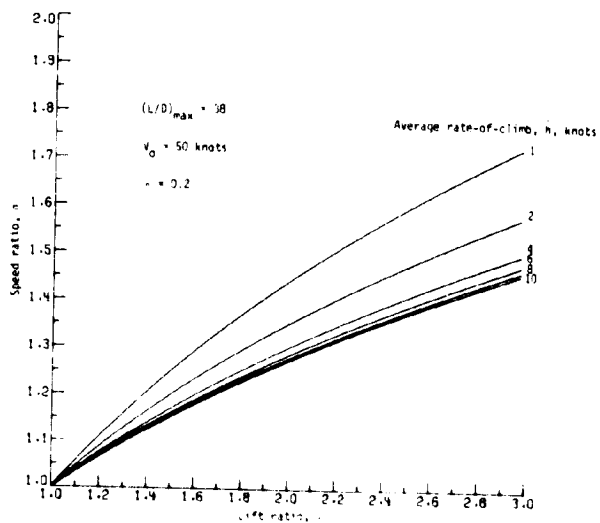
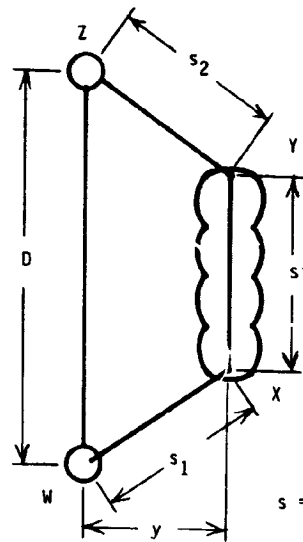


Figure 8. - Speed ratio versus lift ratio for macro-strategy thermal model.



REPRODUCIBILITY OF THE ORIGINAL PAGE IS POOR

$$s = s_1 + s' + s_2$$

Figure 9. - Micro-strategy model with thermal street parallel to course line.

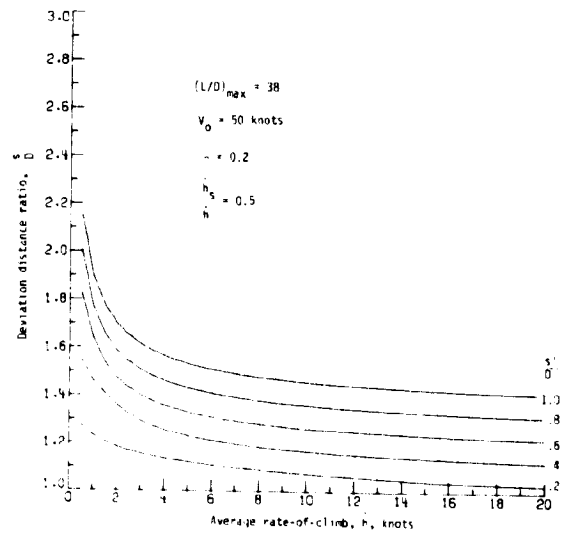


Figure 10. - Deviation distance ratio versus average rate-of-climb for parallel thermal street micro-strategy model.

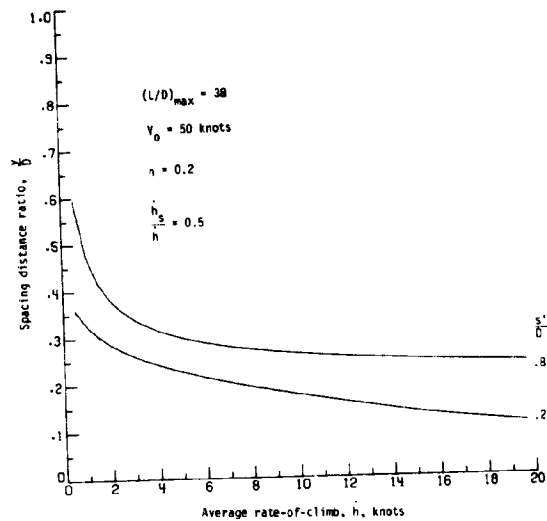


Figure 11. - Spacing distance ratio versus average rate-of-climb for parallel thermal street micro-strategy model.

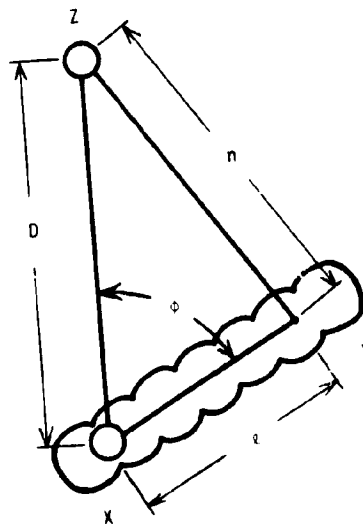
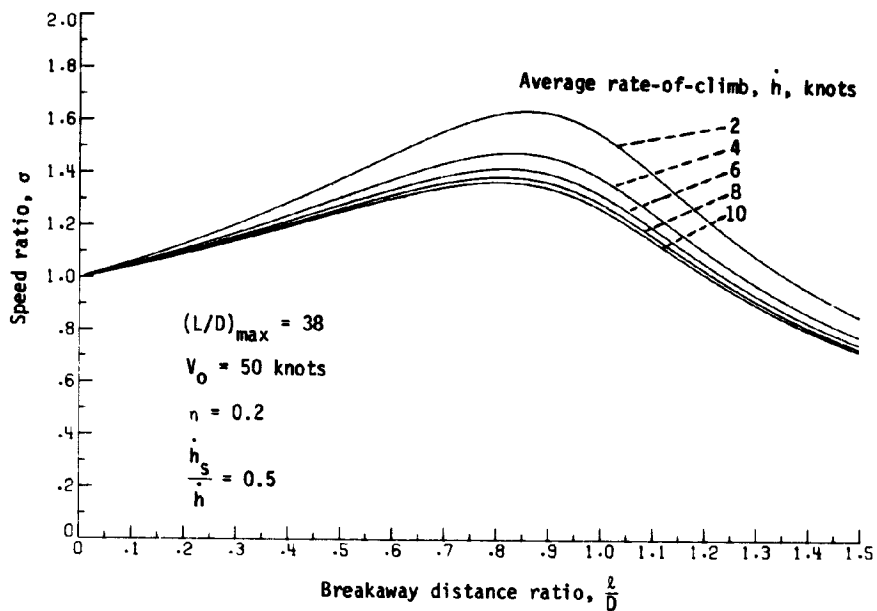
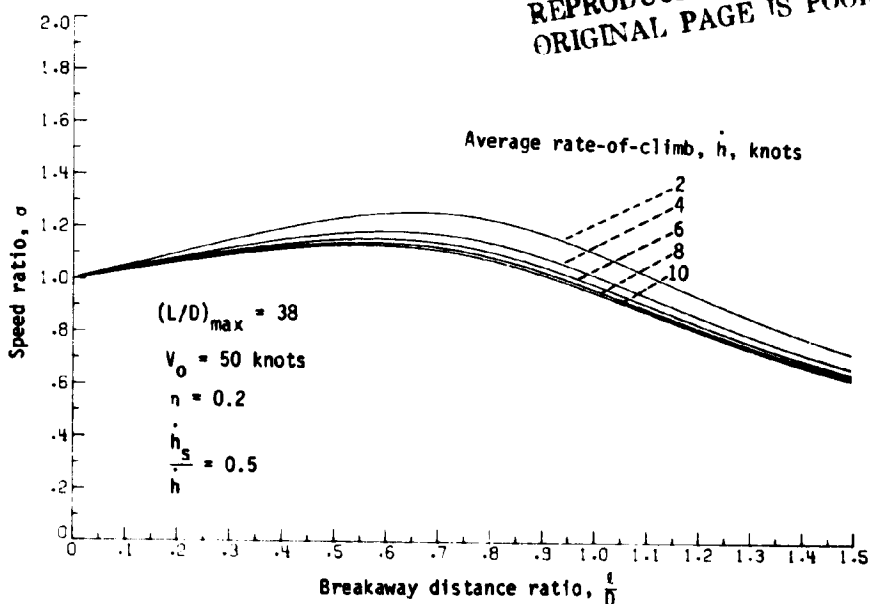


Figure 12. - Micro-strategy model with thermal street at an angle with course line.



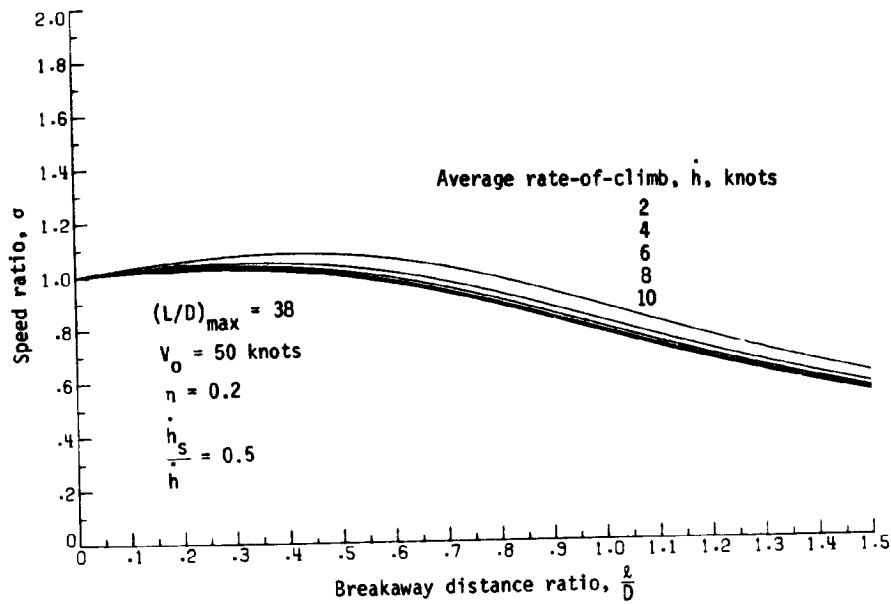
(a) $\phi = 15^\circ$

REPRODUCIBILITY OF THE ORIGINAL PAGE IS POOR

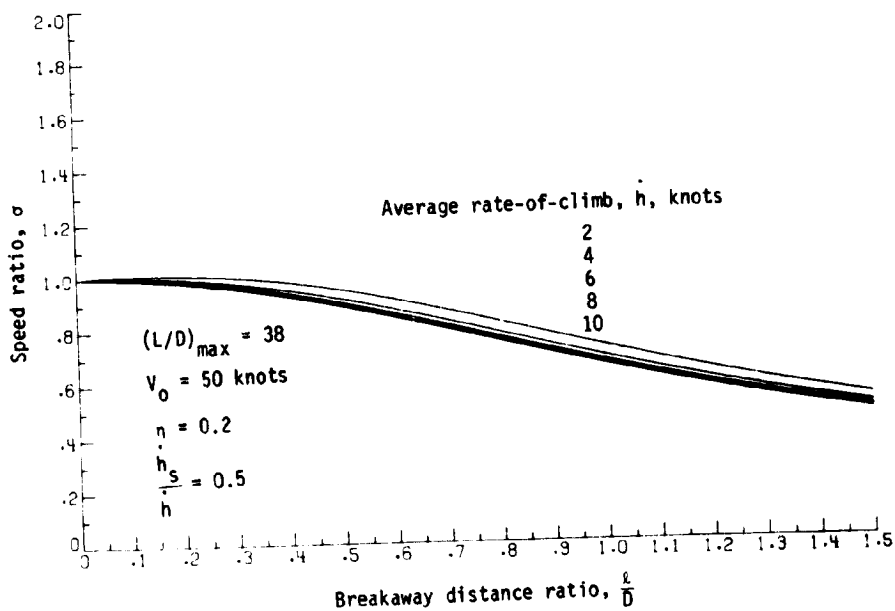


(b) $\phi = 30^\circ$

Figure 13. - Speed ratio versus breakaway distance ratio for a thermal street at an angle to course line.

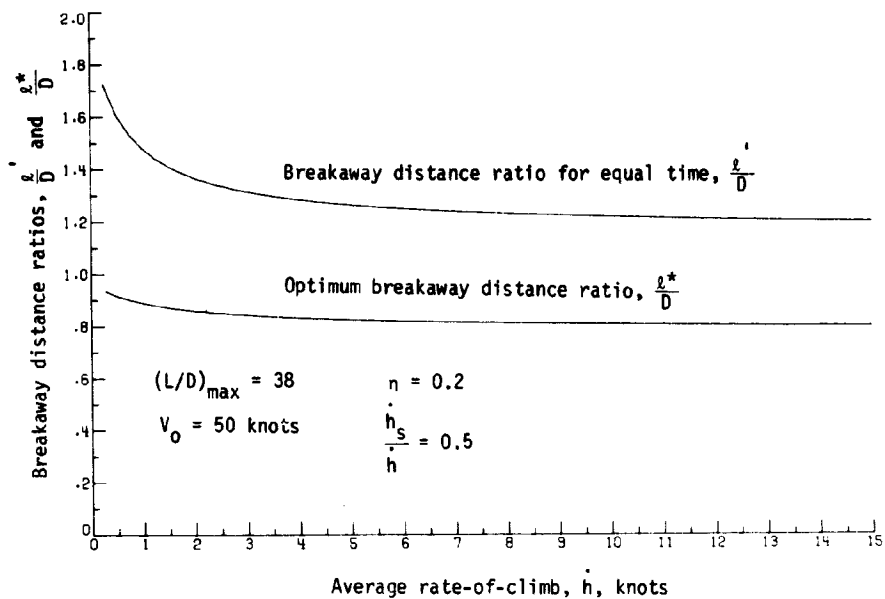


(c) $\phi = 45^\circ$

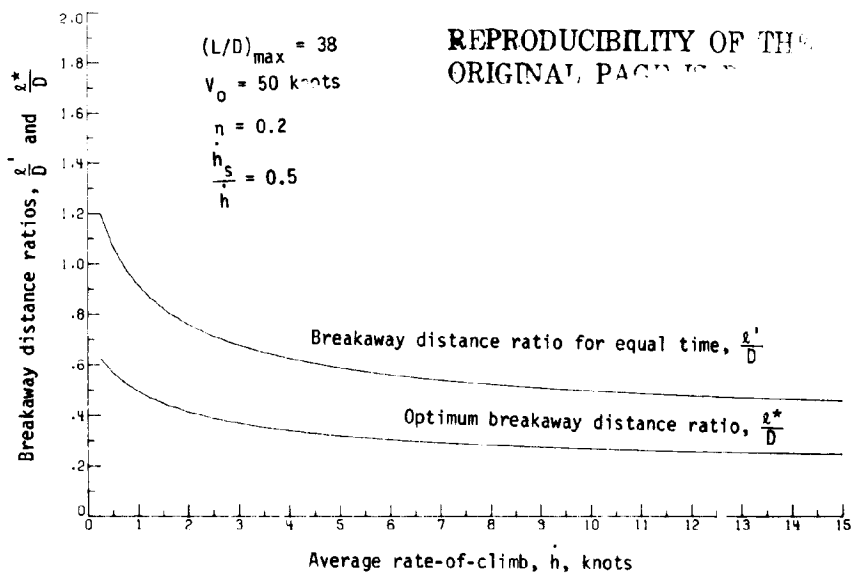


(d) $\phi = 60^\circ$

Figure 13. - Concluded.



(a) $\phi = 15^\circ$



(b) $\phi = 45^\circ$

Figure 14. - Breakaway distance ratios for equal time and optimum time versus average rate-of-climb for a thermal street at an angle to course line.

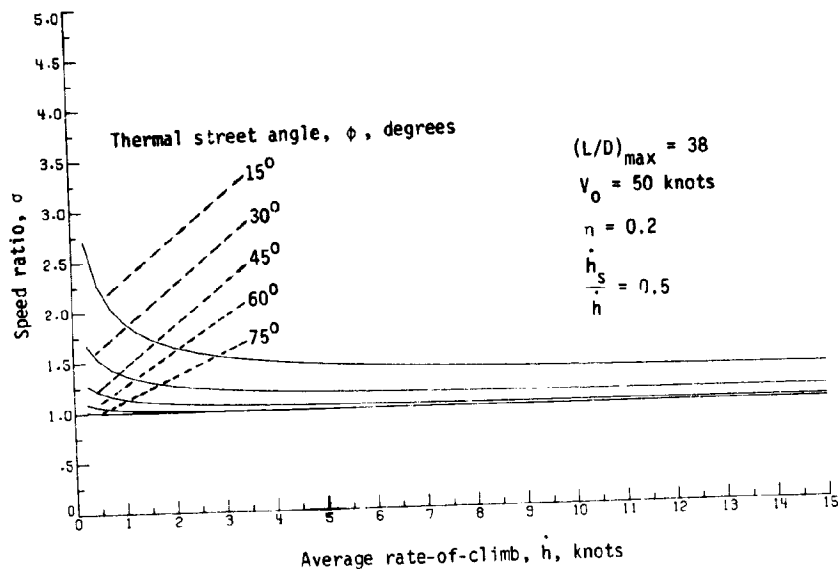


Figure 15. - Speed ratio versus rate-of-climb for a variety of street angles for a thermal street at an angle to course line.

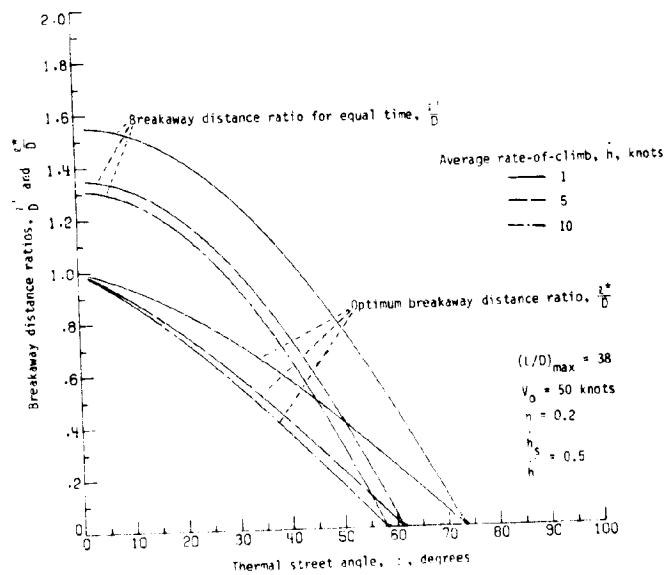


Figure 16. - Influence of thermal street angle upon breakaway distance ratio for a thermal street at an angle to course line.

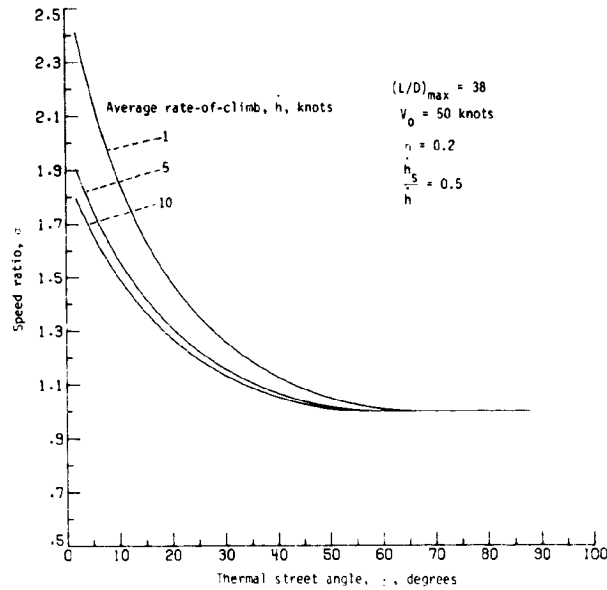


Figure 17. - Speed ratio versus thermal street angle for micro-strategy thermal street model.

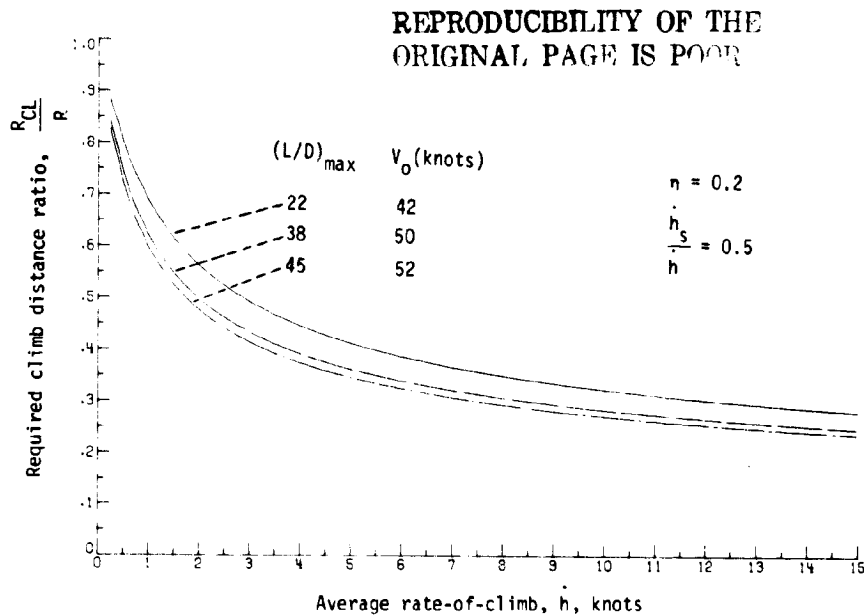


Figure 18. - Required climb distance ratio versus average rate-of-climb for thermal street macro-strategy analysis.

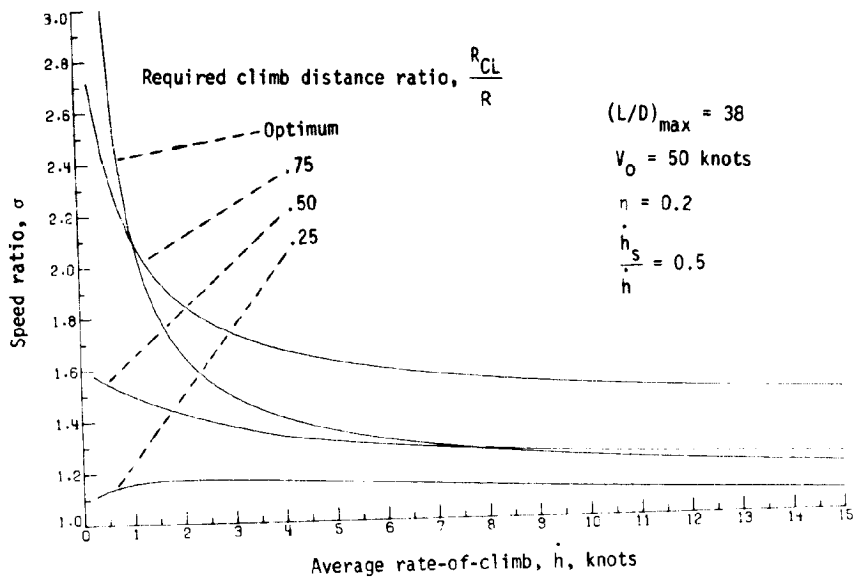


Figure 19. - Speed ratio versus average rate-of-climb for thermal street macro-strategy model.

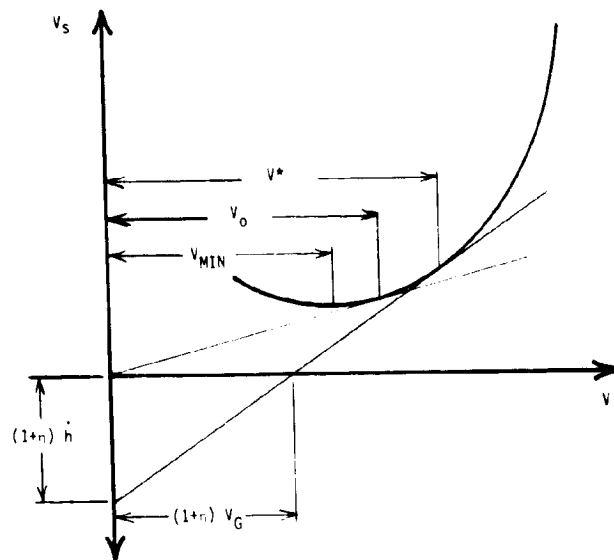


Figure 20. - Sailplane polar showing optimum speed-to-fly constructions for thermal soaring.

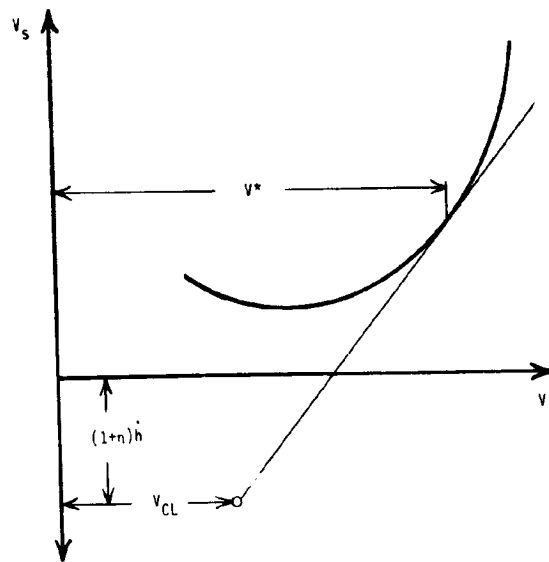


Figure 21. - Sailplane polar showing optimum speed-to-fly constructions for thermal street soaring.

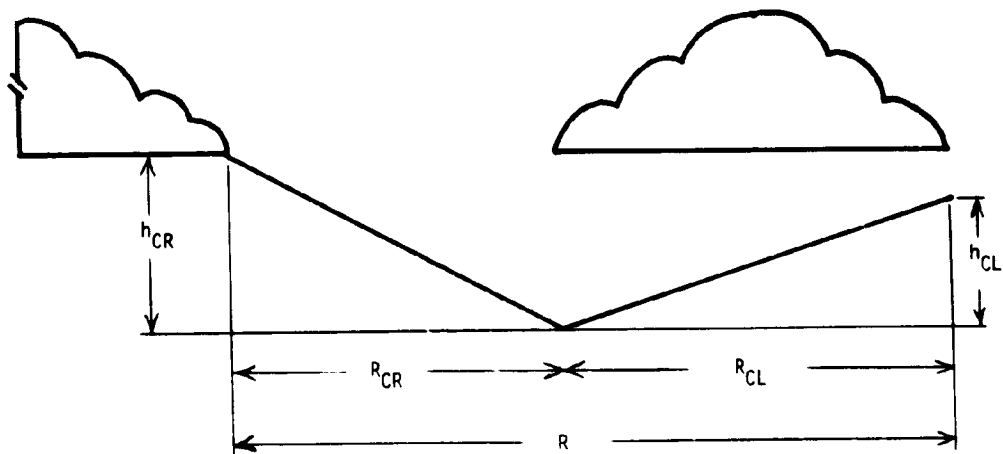


Figure 22. - Flight profile of a glide/climb cycle for thermal street soaring.

23
N79-27073

ON GLOBAL OPTIMAL SAILPLANE FLIGHT STRATEGY

G. Sander and F. X. Litt
University of Liège, Belgium

SUMMARY

The present paper concentrates on the derivation and interpretation of the necessary conditions that a sailplane cross-country flight has to satisfy to achieve the maximum global flight speed. Simple rules are obtained for two specific meteorological models. The first one uses concentrated lifts of various strengths and unequal distance. The second one takes into account finite, non-uniform space amplitudes for the lifts and allows, therefore, for dolphin-style flight. In both models, altitude constraints consisting of upper and lower limits are shown to be essential to model realistic problems. Numerical examples illustrate the difference with existing techniques based on local optimality conditions.

INTRODUCTION

The problems associated with the optimization of sailplane flight paths to achieve maximum cross-country speeds have recently received special attention in the literature. This has been stimulated by the modern competitive soaring which consists almost exclusively in racing and by the development of high performance sailplanes allowing for new, highly efficient flight techniques. Starting with the now classical MacCready [1] results, most of the investigations have been concerned essentially with local optimization problems, that is, finding the optimum flight strategy for various specific situations encountered in a short section of a flight [1 to 10].

In recent papers [2, 4, 5, 8] the optimum speeds to fly in a variety of atmospheric vertical velocity distributions have been determined from the basic assumption that the corresponding flight segments had to be crossed with zero net altitude loss. Conditions under which a transition from the circling mode of climb to the dolphin or essing modes has to be decided have been examined [4]. Although such results yield extremely valuable guidelines for selecting a flight strategy, they only optimize the speed over a limited portion of the total flight.

It is well known, however, in optimization theory that a succession of locally optimum solutions does not, in general, lead to a globally optimum result [11]. It is worth pointing out that a globally optimum flight strategy can only be determined if the assumption is made that the distribution of atmospheric velocities over the whole flight path is known in advance and is independent of time. Although this is never achieved in practice, it is felt that the derivation of global optimality conditions allows for a new insight into the sailplane flight technique by giving a posteriori the decisions that the pilot should have taken and the influence of factors that have